CONFORMED-TO-CAD DESIGN SLOPED-EDGE ADAPTIVE SLICING

Mohammad Hayasi, Bahram Asisbanpour

Ingram School of Engineering, 601 University Drive, Texas State University-San Marcos, 78666, Texas, USA

Abstract

Many mathematical and simulation based researches have shown the effectiveness of adaptive and angular slicing and layering in minimizing errors in layered manufacturing processes and improving surface quality and build time. Recent technological advances such as 5-axis laser cutters, abrasive waterjets, and CNC machines have enabled physical part fabrication beyond typical vertical layered manufacturing with staircase errors. In this paper, a new curved-form adaptive slicing method is presented. In this method, multiple cuts of the edge boundary of each adaptive layer with variable cutting vector angles conform well to CAD model curved surfaces. The proposed system is compatible with 5-axis abrasive waterjet machines. This system has been successfully tested on several virtual 3D CAD models.

1. Introduction

Rapid prototyping (RP) processes, such as direct metal laser sintering (DMLS), fused deposition modeling (FDM), selective laser sintering (SLS), stereolithography (SLA), and 3D printing have been in commercial use for decades across many business sectors. The rapid fabrication of a Computer-aided Design (CAD) model independent of any tooling is appealing as it would significantly reduce time, effort and cost - all crucial factors to the success of any business. To build a rapid 3D prototype that geometrically matches its 3D CAD model, current commercial RP systems often apply very thin layers of metal foil, fine metal/ non-metal powder, or liquid resin laminating from the bottom to top of the CAD model such that steps appearing on the edges of the layered model become less significant. This, however, increases build time and thus fabrication cost. Thick-layer lamination with sloping surfaces offers a possible solution to overcome this problem by reducing the number of layers. Mechanical limitations of the commonly used RP systems make thick-layer building impossible. This is due to the fact that fusing, sintering, soldering, ultrasonic welding, and printing of the dense collection of particles and molecules in any selected bulk region of a variable thick layer is unachievable using present technology. Methods of building functional metallic parts and tooling by means of abrasive waterjet and laser cutting of fully dense metal sheets in various thicknesses followed by alignment and attachment of layers have recently been developed (Nakagawa and Kunieda, 1984; Vouzelaud et al., 1992; Glozer and Bervick, 1992;Walczyk and Hardt ,1996; Bryden et al., 2001; Glen et al., 2011).

The ability to rapidly cut various sheet metal thicknesses from small to large dimensions using abrasive waterjet or laser cutter machines helped to significantly reduce build time

compared to RP approaches that employed very thin layers of material. Fully dense rapid prototypes that are built up from non-uniform (adaptive) layers suffer from staircase errors appearing on the boundary edges of the layered CAD model (Figure 1).
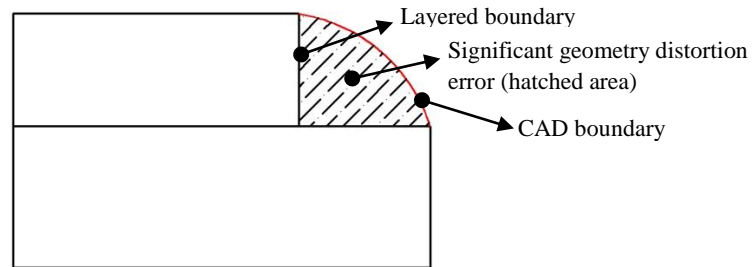
Figure 1. Illustration of the magnitude of geometry deviation error using simple adaptive slicing

The sloped-edge adaptive slicing approach could improve the part quality to some extent but it still results in a geometry distortion error (staircase) even on sloping edges (Figure 2).
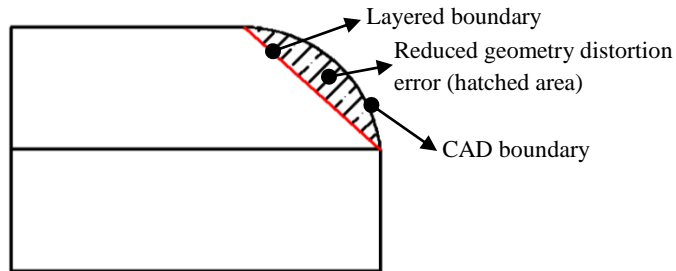
Figure 2. Illustration of the magnitude of geometry deviation error using sloped-edge adaptive slicing

To improve conformity to CAD model geometry, curved-form adaptive slicing on the sloped edges is presented. Multiple cuts of the edge boundary of each adaptive layer at variable cutting angles improve conformity to the CAD model curved surfaces (Figure 3).
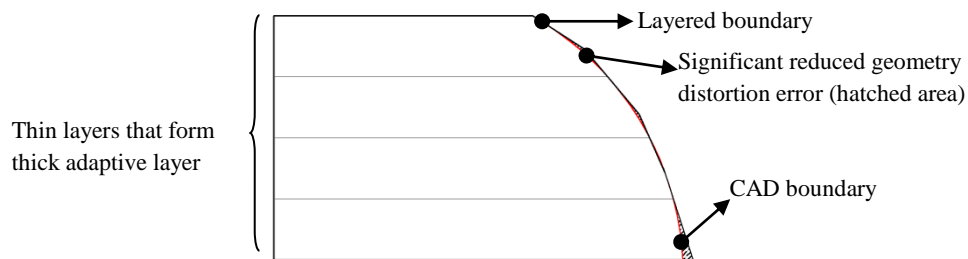
Figure 3. Illustration of the magnitude of geometry deviation error using curved-form adaptive slicing

Adaptive slicing for sloping surfaces takes advantage of applying thicker layers effectively to complex geometrical shapes containing such geometrical characteristics of general 3D models as convex and concave shapes, sudden changes of geometry, ruled surfaces, and sharp edges. In doing so, adaptive slicing, reduces the number of slabs and reduces geometric distortion. For successful implementation of such approaches, more axes of control are required, and the sloping surface path has to be obtained. Sloped-edge adaptive slicing proceeds through

two major steps: determination of the adaptive slice thickness by calculating various geometry deviation errors and connection of the corresponding upper and lower contour points of a layer in order to form the cutting trajectory. In an attempt to build parts with sloping surfaces in RP, Hope et al. (1997a) presented the TruSurf system. This system first takes geometry and topology information from a sample CAD model file in Initial Graphics Exchange Specification (IGES) format. Accessing the B-spline surfaces of the CAD model and parametric data, the system seeks to determine the top and bottom contours resulting from the intersection of the XY plane with the B-spline surface at the defined Z level. Following the determination of the number of contour points defined by the user, the top and bottom contour points are computed by which the continuous connection of points by lines to approximate the actual CAD slices is facilitated. Using this algorithm and simple vector equations, the system succeeded in joining the corresponding top and bottom contour points to create cutting vectors and a trajectory. The linear movement of the 5-axis machine head from start to end points of the connected contour lines and rotational movement of the machine head at two angles in cylindrical coordinates (cutting angle and polar angle) helped to build layers with slanting surface and variable thickness.

Hope et al. (1997b) extended the application of the TruSurf system to the concise determination of variable layer thickness according to the surface geometry complexity. Also, they generated the layer sloping surface either inside the CAD boundary, outside, or a combination of both to meet the finishing requirements of the final prototype by comparing inside and outside tolerances with the computed cusp height. For example, if finishing procedures are to remove material from the prototype surface, the tolerance would fall outside the CAD boundary (cusps of extra materials) resulting in outside inclined ruled surfaces (Figure 4(a)). Conversely if filling material needs to be applied to the surface of the prototype, then the tolerance would fall inside (cusps of missing material) and end up with inside sloped surfaces (Figure 4(b)). Either way requires material deposition or removal post-processing to make the prototype identical to its original CAD model.
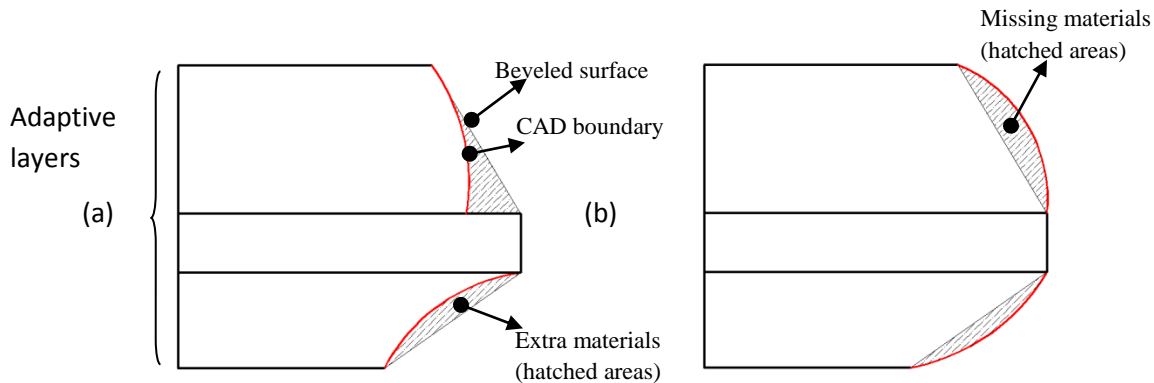

Figure 4. Illustration of outside (a) and inside slicing position (b)

Chamberlain et al. (1998) presented the zero integrated error ruled edge slice (ZIGER slice) algorithm in which cross sections of the sample 3D model are represented in STL format at one degree angle increments giving a total of 359 sections. Sections are first obtained by averaging sample points of facet vertices. The connection of such sample points approximates the slice slope (cutting stream). Then, two important measures of error, average absolute error

and maximum absolute error, contribute to the determination of adaptive thickness slicing. In fact, the above errors were the negative and positive areas emerging between the CAD surface and approximate slope surface (Figure 5).
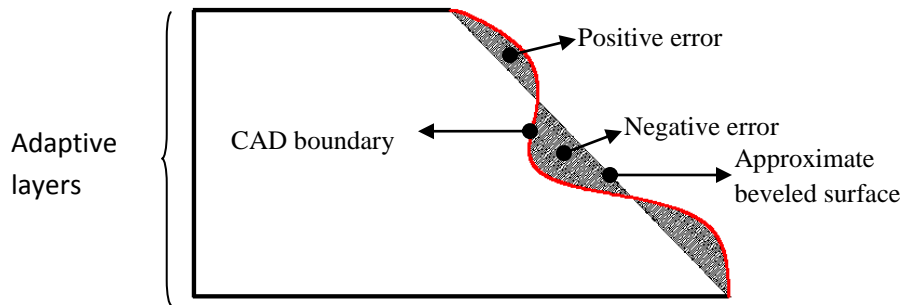

Figure 5. A view of ZIGER slice

Utilizing STL file format, Taylor et al. (2001) computed the intersection of a CAD model represented in STL format with the Z plane at a specified Z value to create a chain of line segments forming the closed-loop or contour. The start and end points of these line segments are swept half the layer thickness above and below the cutting plane to form rectangles in the vertical or slanting depending on the angle of the cutting vector. These rectangles based on the start and end points of a line segment on the created contour and the cutting angle correspond to discreet cutter locations during machining of that contour (Figure 6).
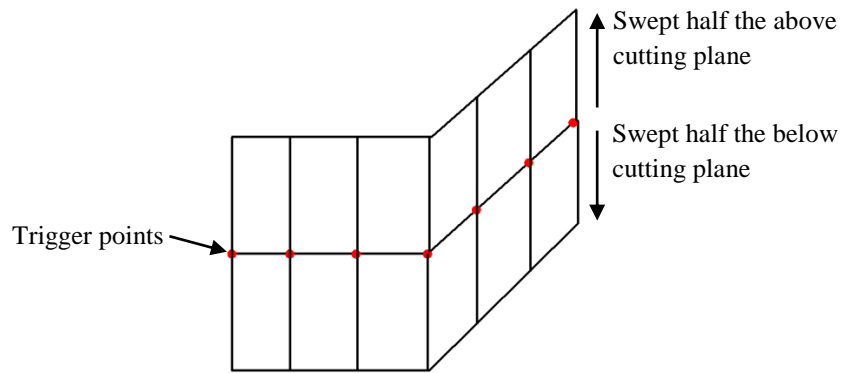

Figure 6. An illustration of cutting trajectory formation.

In conjunction with adaptive ruled layers, Koc and Lee (2002) took into account the generation of ruled surfaces obtained by joining the corresponding top and bottom contour points of an adaptive layer. They concentrated on developing accurate connections of those points such that any twisted surfaces, surface approximation errors, and incorrect contour point joins would be avoided. The algorithm worked well for the connection of top and bottom contour points that were different in number and lent itself to the creation of ruled lines and surfaces, hence easing the generation of machine cutting paths suitable for 5-axis RP (Figure 7).
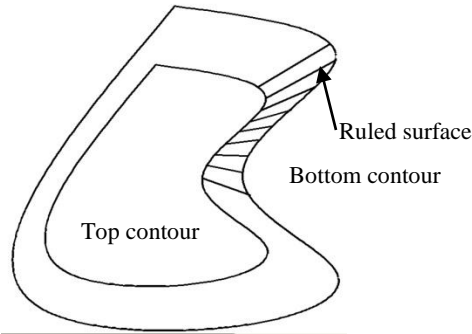
692

Figure 7. Forming the ruled surface.

In another attempt to form ruled surfaces between the contours of an adaptive slice, Gupta et al. (2004) proposed an algorithm to stitch together unequal optimized numbers of top and bottom contour points to obtain acceptable ruled lines, thereby generating well-shaped sloping surfaces and conforming closely to the part surface boundary. Besides computing the optimum number of contour points and developing an adaptive slicing approach, they also provided a solution to the problem of cutting triangle patches that emerged from the multiple connection of one contour point with different points in its corresponding top or bottom contour. Yoo and Walczyk (2005) developed an advanced cutting trajectory algorithm for the profiled edge laminate (PEL) rapid tooling (RT) process (the process of the fabrication of large-scale dies and molds). Instead of slicing a CAD model represented by STL format, they directly performed the slicing process through SolidWorks API. A method for discretization of continuous profiles (i.e. the combination of arcs, splines, parabolas, and ellipsoids) of the CAD model has been developed. To stitch the obtained contour points appearing in front and back profiles for the purpose of accurate PEL surface reconstruction and the creation of optimized cutting vectors, an adaptive surface reconstruction algorithm consisting of Delaunay triangulation and a new complementary stitching algorithm were successfully implemented. The PEL technique is believed to be suitable for thick-layer rapid tooling that is suitable for 5-axis AWJ cutting machines leading to high quality prototypes.

In a nutshell, despite the fact that many endeavors have been carried out in the scope of beveled-edge slicing, no research has been reported to address curved-form lamination for intricate beveled surfaces. Therefore, the possibility of generating accurate machine path enabling curved-form sloped-edge lamination compatible with 5-axis abrasive waterjet (AWJ) cutters will enable fabrication of functional parts from fully dense sheets with geometrical characteristics very near to their original CAD models.

Therefore, the main objective of the present research is to generate sloping surfaces on the edge of an adaptive layer. The resulting surface has much less geometry deviation error and closely fits its CAD model boundary. The proposed system works in the following order: It takes in topology and geometry information from previously generated adaptive layers (Hayasi, Asiabanpour; 2011). Then, the thickness of an adaptive layer and the bottom and top contours of adjacent layers are fed into the proposed algorithm in the form of the continuous connection of vectors and their cutting vector with the facet normal for the creation of curved-form sloping surfaces. Following curved-form adaptive slicing, a customized machine path and CNC code

compatible with 5-axis abrasive waterject cutters will be generated for any user-defined sheet thicknesses.

The remainder of the paper is organized as follows: Section 2 briefly introduces the concept of rapid tooling (RT) and a new RT process named fully dense freeform fabrication (FDFF) with particular focus on metallic functional parts. In line with the quality improvement of the parts cut by the 5-axis abrasive waterjet, details of the new sloped-edge adaptive slicing system are presented in Section 3. Section 4 illustrates customized machine path and CNC-code generation which is consistent with current slicing systems and compatible with 5-axis abrasive waterjets without requiring machine setup modifications. Section 5 deals with implementation of the proposed system. Results achieved by application of the developed software on complex 3D CAD models are presented in Section 6. Finally, future work and conclusions are discussed in section 7.

2. Rapid tooling and fully dense freeform fabrication process

Although the proposed slicing algorithm is applicable to a variety of 5-axis processes that allow variable thickness layering and slicing in different orientations, a brief review of the fully dense freeform fabrication (FDFF) process as the test bed and potential application of this algorithm would give the reader a better insight into the applicability of such an algorithm. The combination of variable thickness layering of any solid material, slicing in different orientations, and bulk layer attachment enables the FDFF process to build good quality complex parts from practically any dense material, including metals, plastic, wood, wax, ceramic, and even glass, at a very fast pace. In this method, a CAD model is sliced into computer layers; the material sheet is then cut from the computer layers. Applying filler material between layers or direct joining of layers followed by layer compression mechanism and heating can be effective techniques to obtain acceptable layer attachment. The type of filler materials (e.g. glue, soldering or brazing filler depending on the applicability of filler material reacting to the heating source) and the acceptable distribution of compressive forces on all layers will be determining factors in attachment quality. Furnace, gas flame, or induction heaters are practical heat sources for heat based bonding methods (Figure 8).
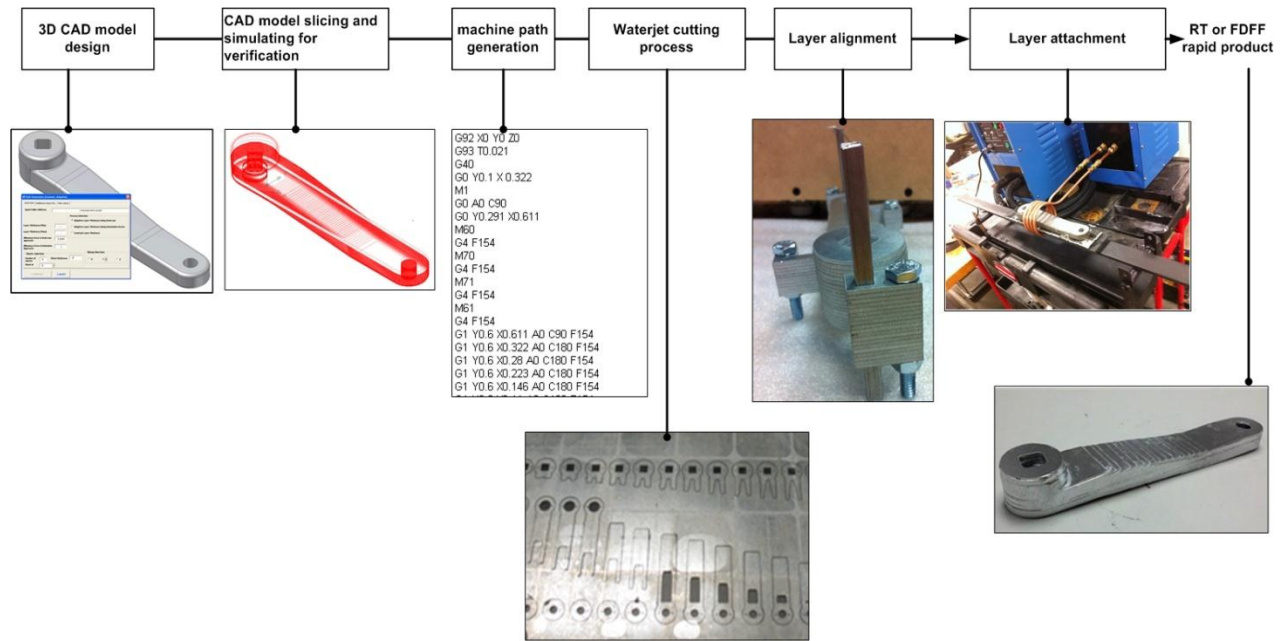
Figure 8. Visualization of the sequences of the FDFF process

Different aspects of the rapid tooling (RT) approaches have been addressed by many researchers such as Nakagawa and Kunieda (1984), Vouzelaud et al. (1992), Glozer and Bervick (1992), Walczyk and Hardt (1996), Bryden et al. (2001), Gibbons et al., (2003), Himmer et al (2003), Perchtl et al. (2005), and Glen et al., 2011.

3. Curved-form adaptive slicing

3-1- Adaptive slicing

The input to curved-form adaptive slicing algorithms is an adaptive slice which carries a limited number of thin layers in order to be assigned an available thick layer. In adaptive slicing the CAD model is initially sliced at the maximum available thickness. Adaptive slicing then applies some specific tolerances to decide whether or not to break the thicker slab down into thinner ones. From this some basic information of a typical adaptive slice such as layer thickness and contour points of the top and the bottom slices of the associated layer are generated. The present system requires topology and geometry information of all thin layers that shape an adaptive slice with the desired thickness (Hayasi and Asiabanpour, 2011).

3-2- Data structure formation for contours

For each layer whether thin (consisting of a bottom and top slice) or thick (encompassing more than two slices), an array of a specific data structure containing the required information for the slices (e.g. the internal and external closed-loop of each slice, the co-planar vectors of each contour, a surface identity assigned to each contour vector, and facet normal vector belonging to each contour vector) will be created. The contours are obtained by the continued connection of vectors or line segments resulting from the intersection of the XY-plane with selected facets at the defined Z level in counter clock-wise (CCW) fashion. Since a contour vector or line segment is the result of connecting two points laid upon the edges of a facet, the

695

identity of a surface extracted from a facet will be readily obtainable by Autodesk Inventor API functions. Furthermore, a facet normal vector is added as an attribute into the data structure of each contour vector as a result of placing start and end points of a line segment on the edges of that facet. Each contour vector is a principle element in the determination of cutting angle and trajectory (Figure 9).

Data Structure (Contour):
1. Start Point (SP)
2. End Point (EP)
3. Contour Vector ($\vec{V}$)
4. Facet normal ($\vec{N}$)
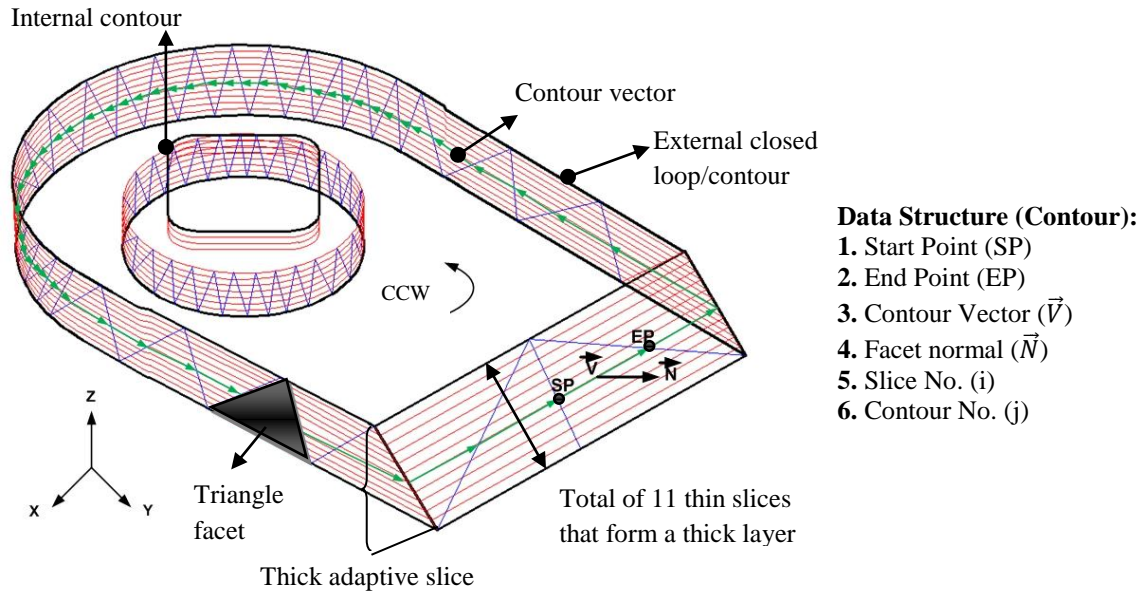5. Slice No. (i)
6. Contour No. (j)

Figure 9. A view of a sample layered model accompanying detail slicing information

Using a contour vector belonging to a specific contour at a sub-slice of the adaptive layer, the system will provide a 5-axis AWJ machine vector movement from vector start to end points, rotational angle (C) around Z axis, and cutting vector angle (A) (Figure 10).
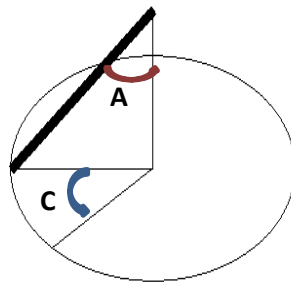

Figure 10. Rotational (C) and cutting (A) angles

The contour vector ($\overrightarrow{C_{ij}}$) is simply obtained by subtracting the end point coordinates from the start point (here i represents a specific slice number within a thick adaptive slice, and j represents an internal/external contour slice within i). Consequently, a cutting vector ($\overrightarrow{V_{ij}}$) can be computed by taking the cross product of the obtained contour vector and a facet normal ($\overrightarrow{N_{ij}}$) that had been added into the vector record in the defined data structure. Since all contour vectors are ordered in counter clock-wise manner, for internal closed-loops (contours) the cross product of

vectors must be given by $\overrightarrow{V_{ij}} = \overrightarrow{C_{ij}} \times \overrightarrow{N_{ij}}$ and by the opposite $(\overrightarrow{V_{ij}} = \overrightarrow{N_{ij}} \times \overrightarrow{C_{ij}})$ for external contours in order to lead the pick of the cutting vector in the direction of the cutting stream. Following calculation of the above vectors, the two rotational and cutting angles are obtained as follows:

Cutting Vector angle: $A = 180 - \cos^{-1} \dfrac{\vec{Z}.\overrightarrow{V_{ij}}}{\|\vec{Z}\|\|\overrightarrow{V_{ij}}\|}$

$$ \text{(1)} $$

Rotational angle: $C = \cos^{-1} \dfrac{\vec{X}.\overrightarrow{V_{ij}}}{\|\vec{X}\|\|\overrightarrow{V_{ij}}\|}$

Figure 11 is a graphic view of the vector computation on the simple adaptive slice including a few thin slices with multiple loops within a thin slice.
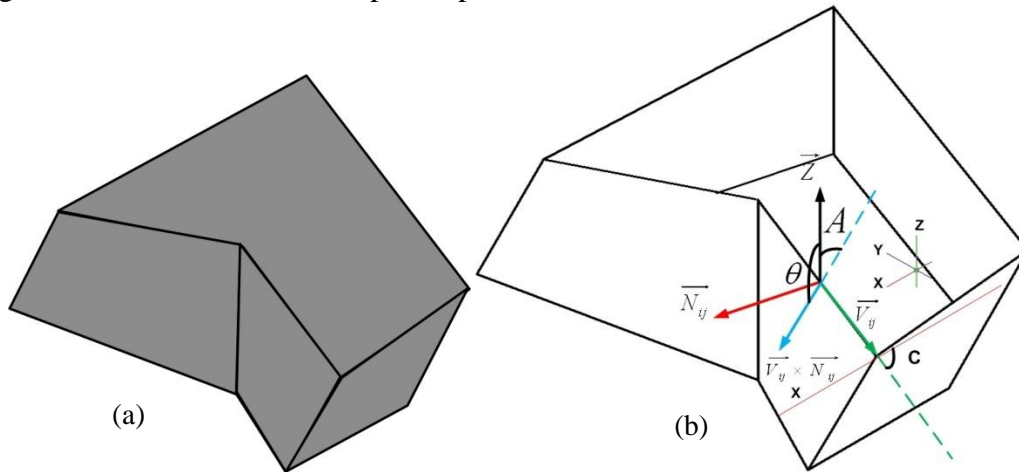

(a)   (b)

Figure 11. A 3D view of CAD model for vector computation (a) visual representation of machine head angles (A,C) and cutting vector (b)

3-3- Cut path difference for convex and concave curves

For cutting curve edges, the proposed system should be capable of recognizing concave or convex curves throughout the surface of the layered model while tracing all contour vectors in a CCW direction. This is an important part of the system as it will help to determine the appropriate action to cut the curved regions. For convex edges, the system will provide a custom machine path along which the multiple cuts required for that edge will be possible. Using multiple cutting vectors for a single convex edge results in a curved-form edge closer to its original CAD edge with minimal geometric deviation (Figure. 12 (a)). For a concave edge, it is impossible to apply multiple cuts in this fashion, as doing so results in removal of excessive material in the first single cut (Figure. 12(b))
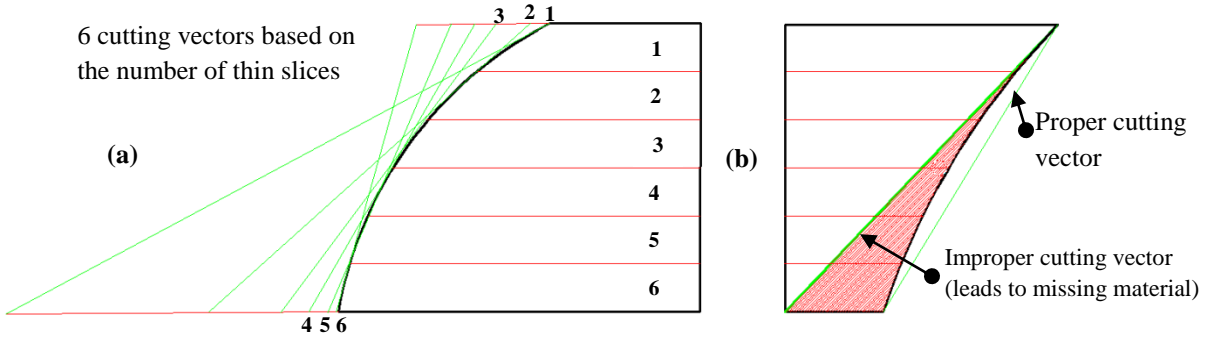
Figure 12. Two cutting strategies: (a) Multiple cuts to form a convex edge (b) single cut for a concave edge

As a result, the top and bottom points of the concave curve and subsequently the connection of these points need to be identified in order to create a single cutting vector, as a guide for the AWJ cutting stream.

3-4- Convex and concave curve identification

In conjunction with the identification of convex and concave edges, a contour vector at a particular slice number, for example, k, is first picked and its start and end points (SP_{kj}, EP_{kj}) and its cutting vector $(\overrightarrow{V_{kj}})$ is extracted from the data structure. Then, the midpoint (MP_{kj}) of SP_{kj}, EP_{kj} is found and mapped onto a plane parallel to the XY-plane and passing through slice number 1. To find a second point that lies on either the concave or convex curve and located on one of the contour vectors of the bottommost slice, a vector $(\overrightarrow{TV_{kj}})$ tangent to the surface at point EP_{kj} is projected on the same plane as the midpoint and a line parallel to that projected vector $(\overrightarrow{PV_{kj}})$ and passing through the projected midpoint (MP_{1j}) is obtained. The points resulting from the intersection of the line (L) with a short list of line segments (lines that surely intersect with the line L) located on the first slice are obtained. Among the points there is a point (IP_{1j}) placed on a contour vector whose surface identity equals that of $\overrightarrow{V_{kj}}$ and also lies on a vector (forming by the candidate point and point MP_{1j}) co-directional with $\overrightarrow{PV_{1j}}$. Once the desired point is obtained, a vector passing through that point and tangent to the part surface is created and its angle (θ) with $\overrightarrow{Z}$ is computed. Again at point MP_{kj} , a vector tangent to the part surface is created and subsequently an angle (β) between this vector and $\overrightarrow{Z}$ is found. A curve edge is regarded as convex if θ is greater than β, otherwise the edge is concave (Figure 13).
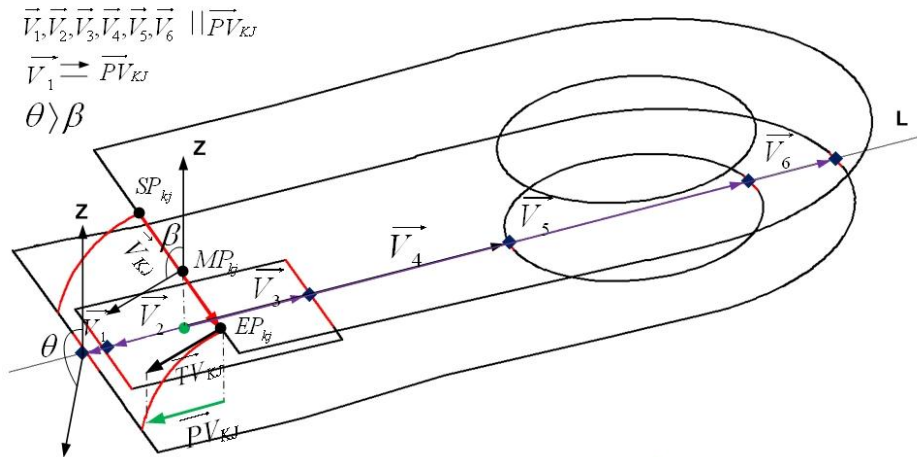
Figure 13. Graphical representation of how a convex edge is identified

3-5- Curved-form adaptive slicing main algorithm

Once the adaptive slicing from the bottom to top of the CAD model is accurately accomplished, an external contour for each adaptive layer containing a number of thin slices is selected from among contours in the top slice of the layer. The initial vector in the chain of the vectors is obtained from the data structure of the contour vectors belonging to the selected contour and the possibility of being convex or concave at this point is evaluated using the method explained above. With regard to concave curves a straight sloping surface is formed by mapping the start and end points of the selected vector onto a plane parallel to the XY-plane and accommodating the contours of the bottom slice. Then two lines passing through the mapped points and parallel with the projected cutting vector of the top contour vector are drawn. The intersection of the lines with the corresponding line segments (contour vectors) on the bottom slice results in two additional points. Eventually, the desired beveled surface, which is created by the connection of those four points, would be a useful tool for both visual simulations of the curved-form cutting and as a source to generate 5-axis AWJ cutter machine trajectories (Figure 14(a)).

Unlike for concave curves the system is required to provide multiple slanting surfaces such that its output conforms to the curvature of convex region. With the assumption that the curvature of the part surface at the initial selected contour vector is found to be convex using the method explained, two lines passing through the start and end point of that vector and parallel to the cutting vector at this location are created. The two lines then intersect with a plane parallel to the XY-plane at a Z-level where the bottom slice is located (Figure 14(b)). The points resulting from the line-plane intersection are simply obtained by the following equation 2.

Line equation: $\dfrac{X-X_0}{a} = \dfrac{Y-Y_0}{b} = \dfrac{Z-Z_0}{c}$, $Z = Z_{slice(k)}$, $Z_0 = Z_{slice(top)}$

X_0, Y_0 are the coordinates of vector's start or end points

$V(a, b, c)$ cutting vector (2)

By setting $t = \dfrac{Z_{slice(k)} - Z_{slice(top)}}{c}$ then $X = X_0 + a \times t$ and $Y = Y_0 + b \times t$
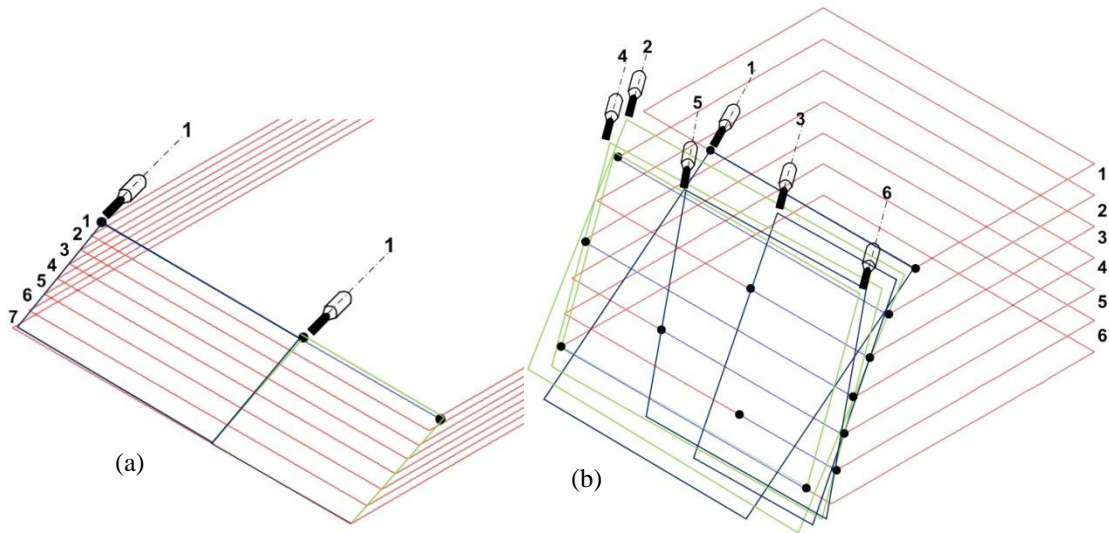
Figure 14. Illustration of a single cutting stream for concave edge (a) and multiple cutting streams for convex edge (b) formed by a number of thin slices

The first slanting surface formed by the connection of the four points is retained in computer memory for further use in machine path generation. To complete beveled surface formation on the top slice, the system seeks to trace all the vectors within either external or internal loops of the slice and apply the above described algorithm. For the remainder of the thin slices, if the curvature of a part surface at a certain vector is found to be concave, the surface formation must be neglected based on the rule defined for such concave curves (i.e. single sloped cutting surface on concave edges). An overview of the developed algorithm presented as a flowchart is shown in Figure 15.
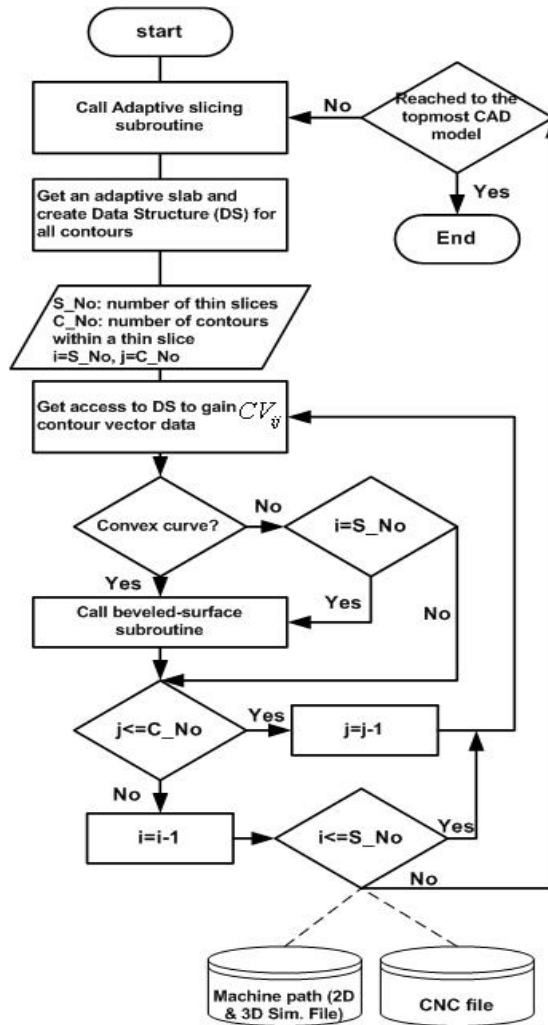
Figure 15. Curved-form adaptive slicing algorithm

4. Machine path and CNC-code generation

Currently available CAD/CAM and CAM systems are not capable of generating code for curved-form 5-axis AWJ multiple cutting paths. Thus some custom modification of G-codes compatible with 5-axis AWJ machines would enable the production of objects very nearly resembling their CAD designs. Since a CAD model is mainly layered in adaptive manner by the use of available sheets on the shop-floor, the size of such sheets must be an input to fit different adaptive slices in their associated sheets according to the sheet thickness. Following CAD model lamination, a group of slices whose thickness falls in the predefined sheet thickness are put together in matrix fashion on the sheet. In order to cut the layers in sequence, the position of each layer on its corresponding sheet is appropriately numbered. The CNC codes are written in such a way that an AWJ machine head would start cutting the layers from the thin through the thick sheet (Figure 16).

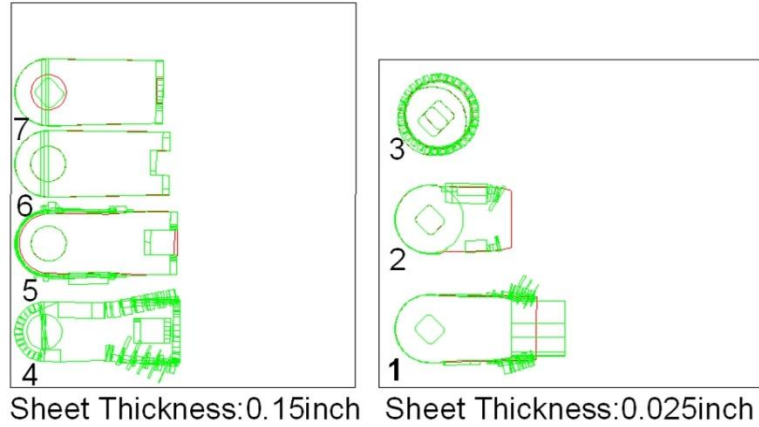Sheet Thickness:0.15inch   Sheet Thickness:0.025inch

Figure 16. Top view of the arrangement of 7 distinct adaptive slices onto two available sheets with specified thicknesses

In G-code generation, there are four basic parameters required for the purpose of 5-axis cutting, namely, linear movement of the machine head from start to end point of each contour vector, rotational and cutting angle of the machine head, and machine feed rate. The first four input data (SP, EP,θ,β) were simply obtained while generating the adaptive slices and applying the foregoing algorithm to each thick layer. There have been a few research efforts to determine how to use machine parameters and cutting depth to assign feed rate to get a good surface roughness quality. As a result, this part of the problem is not in the domain of our research and we mainly refer to previous work that arrived at a comprehensive feed rate formula. The following formula is adopted from the research work of Limbachiya and Patel (2011).

$$v_f = \frac{\pi}{4} d_0^2 R \left(\frac{1}{1+R}\right) 2 \frac{p^{\frac{3}{2}}}{\mu_{job} d_i h_t} \sqrt{\frac{2}{\rho_w}} \qquad \textbf{(3)}$$

Where,

d_0= orifice diameter, d_i= insert diameter, R= ratio of mass flow rate of abrasive to flow rate of water, ρ_w= density of water, μ_{job}= specific energy of material, p= pressure in bar, and h_f=cut depth.

Parameters (d_0,d_i, R, ρ_w, μ_{job}, and p) are easily obtained, but to calculate h_f we must measure the depth of either vertical or slanting surfaces at every contour vector position on the adaptive layer. The calculation of h_f is graphically depicted in Figure 17.
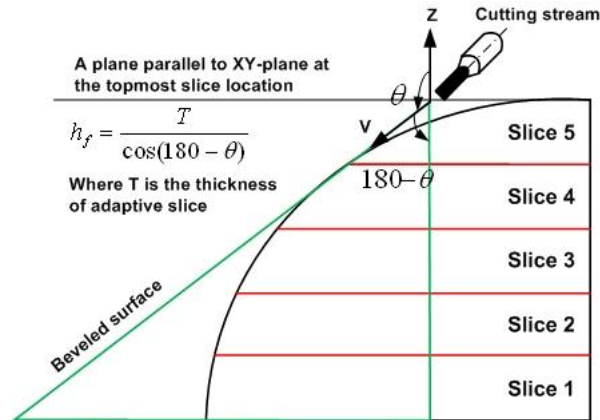
Figure 17. The explicit computation of h_f in the projected view of a sample adaptive slice

5. System implementation

The algorithm was implemented using Visual Basic for Application (VBA) and Autodesk Inventor mechanical design software. Autodesk Inventor API functions were used to gain direct access to topology and geometry information of any complex CAD model. A user interface form facilitates data entries (i.e., slice direction in either X, Y, or Z directions, various sheet thicknesses, allowable errors for boundary area deviation, triangle area, number of available sheets, sheets thickness, and the width and length of the sheets). Figure 18 illustrates the user interface form for triple slicing approaches that was developed in response to a user request. Even though the generated 5-axis AWJ machine codes are saved in one text file, the software output can be obtained layer by layer in the 2D and 3D versions. In the 2D version, the generated layers containing line segments and sloping surfaces are grouped according to their sheet thickness and spread on the sheet rectangle surfaces in matrix form followed by numbering each adaptive slice. In contrast, in the 3D version all layers along with their cutting surfaces in their own thickness are stacked together in the build direction to form an approximate real 3D solid model for better visualization of the final physical part being fabricated by the FDFF process.
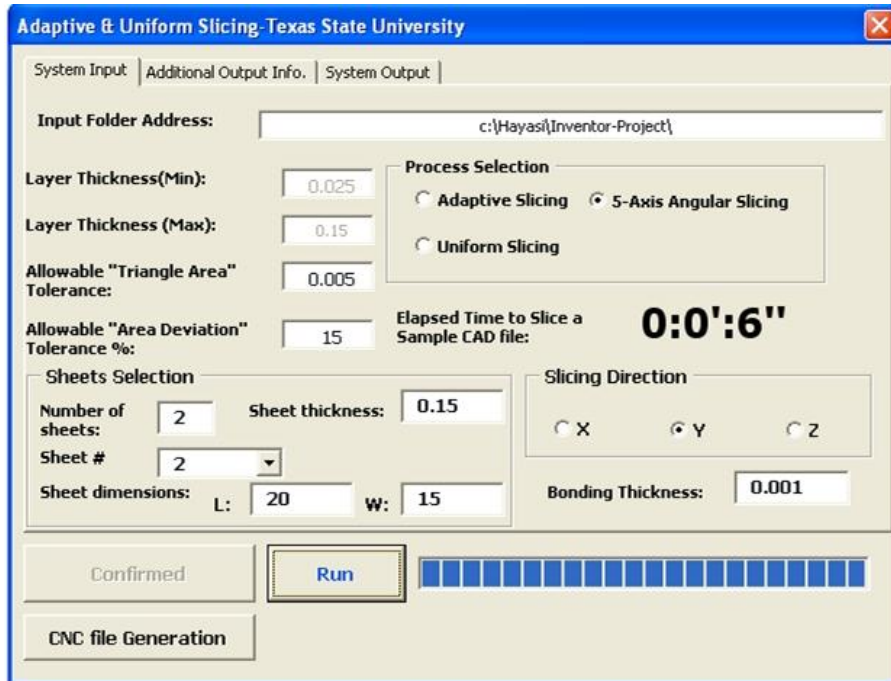
Figure 18. The user interface form.

6. System results, verification, and validation

The implemented system was successfully tested for slicing a variety of models with diverse types of surfaces (i.e., flat, convex, and concave), different slicing direction, and different number of sheets with different thicknesses. The following example along with different stages of the curved form adaptive slicing is presented below:

The entries for model were: sheet thicknesses and sizes T1: 0.1 in, L1: 20 in, W1: 15 in, T2: 0.25 in, L2: 15 in, W2: 30 in, and Cut direction: Z (Figure 19)
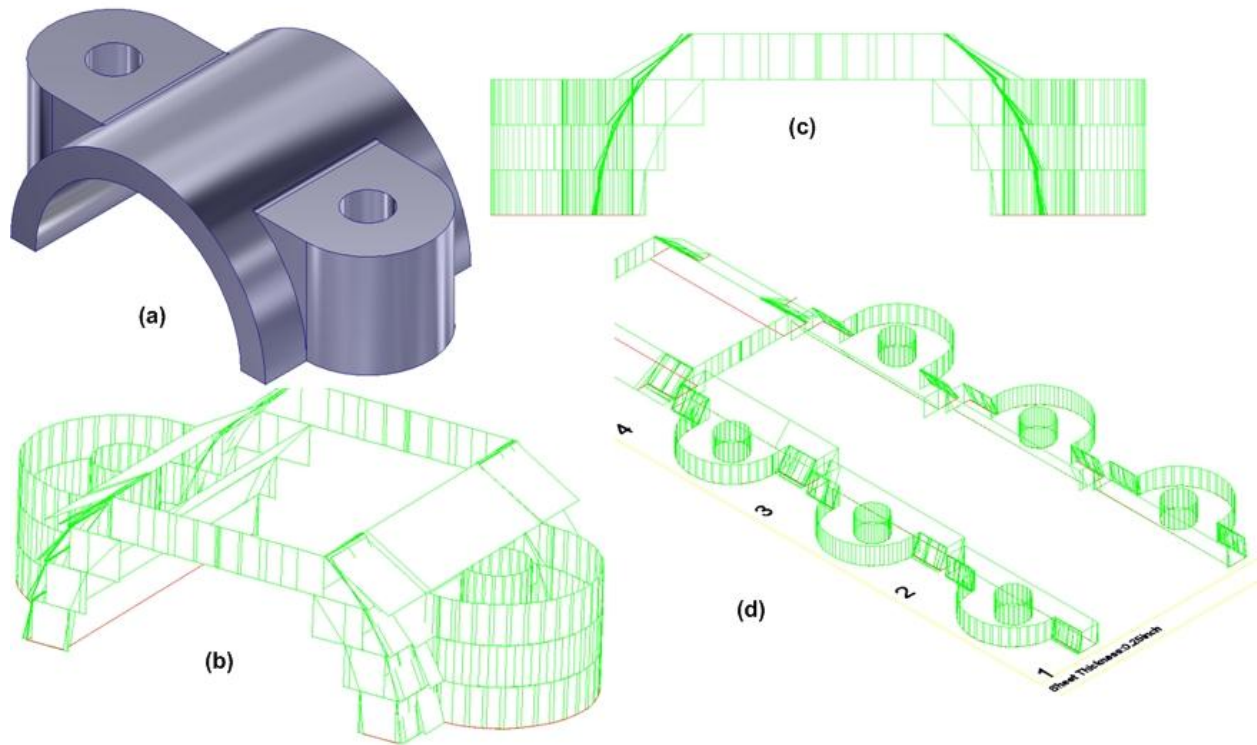
Figure 19. (a) 3D CAD model and (b-d) 3D and side view of curved-form adaptive slicing

7- Conclusion

In this article a new curved-form adaptive slicing method is presented. In this method, multiple cuts of the edge boundary of each adaptive layer with variable cutting vectors angles conform well to the CAD model curved surfaces. The results showed that the staircase effect, a common error in adaptive slicing, existing on either concave or convex edges has been significantly reduced utilizing this method. The proposed system is compatible with 5-axis abrasive waterjet machines. This system has been successfully tested on several models. The main application of the proposed system is in the FDFF process. Metallic sheets with variety of predefined thicknesses can be cut with angular direction by a 5-axis AWJ machine and according to the tool path generated by the proposed system. Then, layers are aligned and bonded in the FDFF process. The bonding process is typically by the induction heater and by using the brazing materials. Therefore, the mechanical properties of the fabricated parts are good enough to be used as the functional parts. The FDFF process has been extensively used and tested for the parts cut by a 2 axis AWJ machine. The future of this research is the test of the FDFF process for the parts cut by a 5 axis AWJ machine, subject to purchase/access.

References

Asiabanpour, B., & Khoshnevis, B. (2004). Machine path generation for the SIS process. Robotics and Computer-Integrated Manufacturing, 20, 167–175.

Bryden, B.G., Wimpenny, D.I., & Pashby I.R. (2001). Manufacturing Production tooling using metal laminations. Rapid Prototyping Journal, 7(1):52-59.

Chamberlain, P.B., Van Rossendaal, M.D., & Thomas, C.L. (1998). Variable thickness ruled edge slice generation and three-dimensional graphical error visualization. Proceedings of the Solid Free Fabrication Symposium, August (1998), 311–318.

Gibbons, G.J., Hansell, R.G., Norwood, A.J., & Dickens P.M. (2003). Rapid laminated die-cast tooling. Rapid Prototyping Journal, 23(4):372-381.

Glen, T.C., Loerwald, M., Hayasi, M., & Asiabanpour, B. (2011). Layer Alignment and Lamination for the Fully Dense Freeform Fabrication (FDFF) Process. 22nd International Solid Freeform Fabrication (SFF) Symposium, Austin, TX.

Glozer, G. R., & Brevick, J. R. (1992). Laminate tooling for injection molding. Proceedings of the Institution of Mechanical Engineers, Part B: Journal of Engineering Manufacture, 207, 9-15.

Gupta, T., Chandila, P.K., Tripathi, P., & Roy Choudhury, A. (2004). Direct slicing with optimum number of contour points. International Journal of CAD/CAM, 4(1):1-2.

Hayasi, M., & Asiabanpour, B. (2011). "Adaptive Direct Slicing and Machine Path Generation for the Fully Dense Freeform Fabrication (FDFF) Process with the Variable Layers", 22nd International Solid Freeform Fabrication (SFF) Symposium, Austin, TX, 2011.

Himmer, T., Techel, A., Nowotny, S., & Beyer, e. (2003). Recent developments in metal laminated tooling by multiple laser processing. Rapid Prototyping Journal, 9(1):24-29.

Hope, R. L., Jacobs, P.A., & Roth, R.N. (1997). Rapid prototyping with sloping surfaces. 1. Rapid Prototyping Journal, 3(1): 12-19.

Hope, R. L., Roth, R. N., & Jacobs, P.A. (1997). Adaptive slicing with sloping layer surfaces. 2. Rapid Prototyping Journal, 3(3): 89-98.

Koc, B., & Lee, Y.S. (2002). Adaptive Ruled Layers Approximation of STL Models and Multiaxis Machining Applications for Rapid Prototyping. Journal of Manufacturing Systems, 21(3):153-166.

Limbachiya, V.J., & Patel, D.M. (2011). An Investigation of Different Material on Abrasive Water jet Machine. International Journal of Engineering Science and Technology (IJEST), 3(7):5940-5945.

Nakagawa, T., & Kunieda, M. (1984). Manufacturing of laminated deep drawing dies by laser beam cutting. Advanced Technology of Plasticity, Vol. 1.

Taylor, J.B., Cormier, D.R., Joshi, s. & Venkataraman, V. (2001). Contoured edge slice generation in rapid prototyping via 5-axis machining. Robotics and Computer Integrated Manufacturing, 17:13-18.

Vouzelaud, F.A., Bagchi, A., & Sferro, P.F. (1992). Adaptive laminated machining for prototype dies and molds: part I and II. Proceedings of the 3rd Symposium in Solid Freeform Fabrication, Austin, TX.

Vouzelaud, T., & Bagchi, A. (1995). An adaptive lamina generation for shape dependent process control and/or object decomposition. Patent number: 5,432,704.

Walczyk, D. Hardt. (1996). Recent developments in profiled-edge lamination dies for sheet metal forming. Proceedings of the Seventh Solid Freeform Fabrication Symposium, Austin, TX.

Yoo, S., & Walczyk, D. (2005). An advanced cutting trajectory algorithm for laminated tooling. Rapid Prototyping Journal, 11:199-213.